Dev Genes Evol
DOI 10.1007/s00427-013-0463-7

ORIGINAL ARTICLE

Patterns of molecular evolution of the germ line specification gene *oskar* suggest that a novel domain may contribute to functional divergence in *Drosophila*

Abha Ahuja · Cassandra G. Extavour

Received: 10 September 2013 / Accepted: 7 December 2013

Abstract In several metazoans including flies of the genus *Drosophila*, germ line specification occurs through the inheritance of maternally deposited cytoplasmic determinants, collectively called germ plasm. The novel insect gene *oskar* is at the top of the *Drosophila* germ line specification pathway, and also plays an important role in posterior patterning. A novel N-terminal domain of *oskar* (the Long Oskar domain) evolved in Drosophilids, but the role of this domain in *oskar* functional evolution is unknown. Trans-species transgenesis experiments have shown that *oskar* orthologs from different *Drosophila* species have functionally diverged, but the underlying selective pressures and molecular changes have not been investigated. As a first step toward understanding how Oskar function could have evolved, we applied molecular evolution analysis to *oskar* sequences from the completely sequenced genomes of 16 *Drosophila* species from the *Sophophora* subgenus, *Drosophila virilis* and *Drosophila immigrans*. We show that overall, this gene is subject to purifying selection, but that individual predicted structural and functional domains are subject to heterogeneous selection pressures. Specifically, two domains, the *Drosophila*-specific Long Osk domain and the region that interacts with the germ plasm protein Lasp, are evolving at a faster rate than other regions of *oskar*. Further, we provide evidence that positive selection may have acted on specific sites within these two domains on the *D. virilis* branch. Our domain-based analysis suggests that changes in the Long Osk and Lasp-binding domains are strong candidates for the molecular basis of functional divergence between the Oskar proteins of *D. melanogaster* and *D. virilis*. This molecular evolutionary analysis thus represents an important step towards understanding the role of an evolutionarily and developmentally critical gene in germ plasm evolution and assembly.

Keywords *Drosophila* · Positive selection · Oskar · Germ line specification · Germ plasm · Novelty

Communicated by: Claude Desplan

Electronic supplementary material The online version of this article (doi:10.1007/s00427-013-0463-7) contains supplementary material, which is available to authorized users.

A. Ahuja (✉) · C. G. Extavour (✉)
Department of Organismic and Evolutionary Biology, Harvard University, 16 Divinity Avenue, Cambridge, MA 02138, USA
e-mail: abha_ahuja@hms.harvard.edu
e-mail: extavour@oeb.harvard.edu

Present Address:
A. Ahuja
Curriculum Fellows Program, Department of Cell Biology, Harvard Medical School, Boston, MA, USA

Introduction

The advent of a dedicated germ line is a major evolutionary transition associated with the origin of multicellularity (Michod 2005). In all sexually reproducing animals, the specification of the germ line early in embryogenesis is a critical developmental event. Two modes of germ line specification have been identified in metazoans: inheritance of maternally synthesized cytoplasmic germ line determinants (germ plasm), and the induction of germ cell fate by signals from neighboring somatic cells (Extavour and Akam 2003). Phylogenetic analyses of these developmental patterns suggest that the inductive mode may be ancestral in metazoans, with germ plasm-driven mechanisms having evolved independently in multiple lineages (Extavour and Akam 2003; Blackstone and Jasker 2003). In *Drosophila melanogaster*, germ cells are specified by the inheritance mode, and germ plasm is assembled during oogenesis by the products of the *oskar* gene. Oskar protein physically interacts with and recruits germ plasm components, including Valois, Lasp, and Vasa proteins

Published online: 10 January 2014

and *nanos* mRNA (Ephrussi et al. 1991; Breitwieser et al. 1996; Suyama et al. 2009; Cavey et al. 2005). *oskar* is necessary and sufficient for germ plasm assembly (Ephrussi and Lehmann 1992), and because it localizes the posterior determinant *nanos*, it is also required for posterior body patterning (Ephrussi et al. 1991).

Surprisingly, in contrast to most other critical metazoan germ line genes, *oskar* is not highly conserved across animals. It is instead a novel gene that evolved in the lineage leading to insects (Ewen-Campen et al. 2012), and may have facilitated the evolution of germ plasm in holometabolous insects (those that undergo true metamorphosis) (Lynch et al. 2011). *oskar* orthologs have been identified to date only from flies and mosquitoes (Diptera, the furthest derived clade of holometabolous insects) (Goltsev et al. 2004; Juhn and James 2006; Juhn et al. 2008), ants and wasps (Hymenoptera, the most basally branching clade of the Holometabola) (Lynch et al. 2011), and a basally branching hemimetabolous insect, the cricket *Gryllus bimaculatus* (Ewen-Campen et al. 2012). *oskar* is absent from the genomes of multiple holometabolous insects that lack germ plasm, including the silk moth *Bombyx mori*, the beetle *Tribolium castaneum*, and the honeybee *Apis mellifera*, indicating that this gene has been secondarily lost several times in holometabolous evolution (Lynch et al. 2011).

The domain organization of *oskar* (Fig. 1a) further underscores the dynamic evolutionary history of this gene. Three domains are common to all known *oskar* orthologs. The first is a predicted N-terminal RNA-binding LOTUS domain, which is also present in the highly conserved Tudor domain family members Tdrd5 and Tdrd7 (Callebaut and Mornon 2010; Anantharaman et al. 2010). However, *oskar* lacks Tudor domains, and is thus not a subclass of Tudor family genes (Lynch et al. 2011). The second is a C-terminal domain that shares greatest sequence and physicochemical similarity to SGNH class hydrolases, an ancient group of lipid-interacting proteins present in all kingdoms of life (Juhn et al. 2008). Finally, part of the region between the LOTUS and SGNH domains has been shown to interact with the actin-binding protein Lasp in *D. melanogaster* (Suyama et al. 2009). In contrast to these three relatively conserved domains, the N-terminal-most domain, called Long Osk, is completely absent in mosquito, hymenopteran, and cricket *oskar* orthologs, and is thus likely an innovation that arose at some point after the divergence of the lineages leading to *Drosophila* and mosquitoes (approximately 260 Mya) (Gaunt and Miles 2002).

Even within Drosophilids, *oskar* has diverged functionally (Fig. 2). In some cases, *oskar* function appears highly conserved. For example, the *oskar* ortholog from *D. immigrans (immosk)*, which diverged from the *D. melanogaster* lineage 30–60 Mya (Remsen and O'Grady 2002; Obbard et al. 2012), can rescue germ cell and body patterning defects of *D. melanogaster oskar* null mutants (Jones and Macdonald 2007). *D. melanogaster oskar* null flies carrying an *immosk* transgene display pole plasm morphology more similar to that of *D. immigrans* than that of *D. melanogaster*, but this pole plasm still contains the conserved germ plasm component Aubergine and is sufficient to form germ cells (Jones and Macdonald 2007). This indicates that although *immosk* may function differently from *D. melanogaster oskar* with respect to the specific morphology of the germ plasm that it confers, *immosk*-like germ plasm is still sufficient to induce germ cell formation in *D. melanogaster*, indicating essential functional conservation between *immosk* and *D. melanogaster osk* with respect to a role in germ cell formation.

In contrast, *oskar* from the equally distantly related species *Drosophila virilis (virosk)* does not show functional conservation of its germ plasm role in a *D. melanogaster* context. In *D. virilis*, *virosk* transcript is localized to the posterior pole of oocytes and embryos like its homolog in *D. melanogaster* (Webster et al. 1994). *D. virilis* embryos also form posterior germ plasm and subsequently pole cells (Webster et al. 1994), suggesting that the germ plasm function of *oskar* is conserved in *D. virilis*, as in *D. immigrans*. In transgenic *D. melanogaster oskar* loss of function mutants carrying a *virosk* transgene, Virosk appears to recruit sufficient *D. melanogaster nanos* mRNA to rescue posterior patterning in these mutants (Webster et al. 1994). However, in *D. melanogaster*, Virosk is unable to assemble functional germ plasm, and thus unable to direct germ cell formation (Webster et al. 1994). This suggests that although Virosk may retain some ability to interact with *D. melanogaster nanos* mRNA, its interactions with other *D. melanogaster* germ plasm components may be too divergent to permit assembly of functional pole plasm in a *D. melanogaster* context, indicating essential functional divergence. Given that *oskar's* role in functional germ plasm assembly appears conserved even in Hymenoptera (Lynch et al. 2011), it is likely that *virosk* and *immosk* direct functional germ plasm assembly in *D. virilis* and *D. immigrans* respectively, via interactions with the germ plasm component orthologs in these species. In this paper, we focus on the functional divergence within the genus *Drosophila* that prevent Virosk's fruitful interaction with *D. melanogaster* germ plasm gene products, despite the high level of conservation of most other germ plasm genes (Ewen-Campen et al. 2010).

Although *oskar* plays an indispensible role in Drosophilid germ cell specification, the nature of the selective pressures and molecular changes responsible for its functional divergence within the genus *Drosophila* are unknown. To gain insight into the molecular evolution of this novel and critical gene, we took advantage of the completely sequenced genomes of 16 *Drosophila* species from the *Sophophora* subgenus, the *D. virilis* genome sequence and the sequenced *oskar* locus from *D. immigrans*. The goal of this study is to assess patterns of change in the *oskar* nucleotide sequence to evaluate potential variation in the evolutionary rate of distinct functional protein domains. We test the hypothesis that

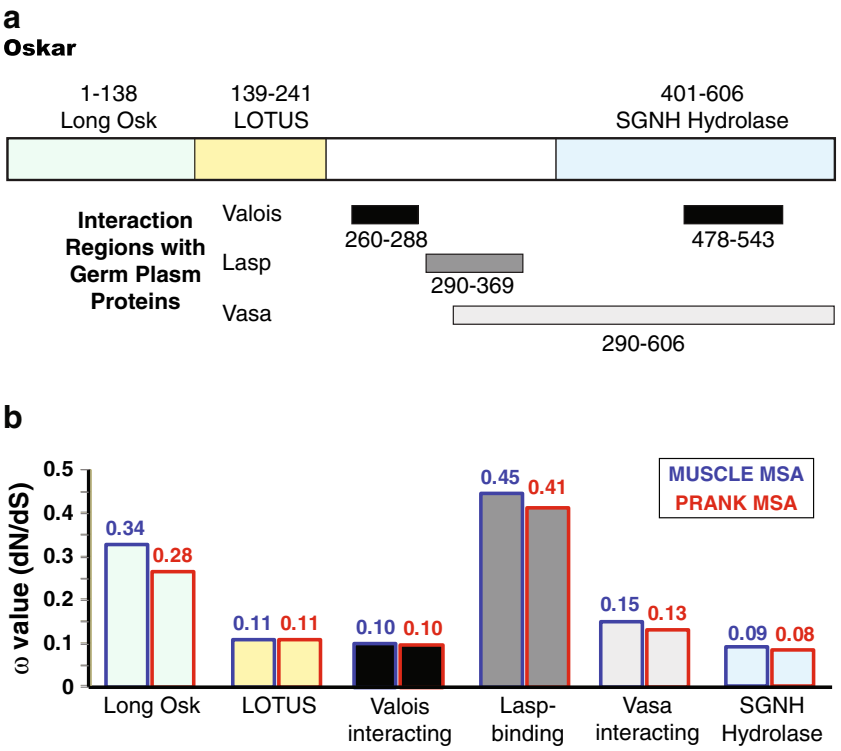

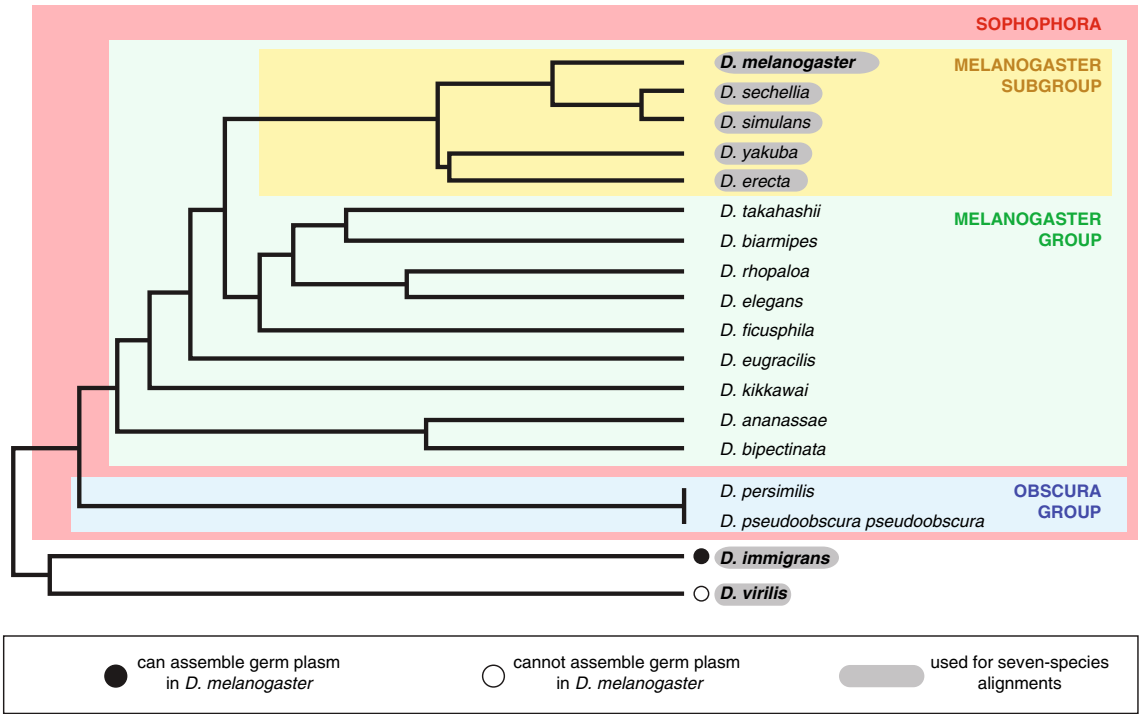

Fig. 1 **a** Domain organization of *Drosophila* Oskar. Amino acid residues corresponding to the *Drosophila*-specific Long Osk domain (*green*), conserved predicted structural domains (LOTUS: *yellow*; SGNH hydrolase: *blue*), and regions shown to interact with conserved germ line specification genes in *D. melanogaster* (*gray shades*) are indicated. **b** ω value estimates for *oskar* predicted structural and interaction domains from combined maximum likelihood analysis based on two different MSA methods using fixed sites model E. Valois-interacting domains were concatenated for analysis

Fig. 2 Phylogenetic tree of *Drosophila* species showing topology used for PAML analysis, which is essentially consistent with current phylogenetic hypotheses (Yang et al. 2012; Kopp 2006). Species where functional analysis of *oskar* has been performed (Webster et al. 1994; Jones and Macdonald 2007) are indicated in *bold*. *D. immigrans oskar* shows functional conservation with respect to germ plasm assembly in *D. melanogaster* (*black circle*), whereas this *oskar* function has diverged in *D. virilis* (*white circle*). The 18 species analyses used *oskar* sequences from all species shown; the seven species analyses used sequences from those species outlined in *gray*, and the five species analyses used sequences only from the *melanogaster* subgroup species (*yellow box*)

positive selection drives the evolution of *Drosophila oskar*, and identify regions that are likely to underlie functional divergence between *D. virilis* and *D. melanogaster oskar*, providing candidates for future study of the evolutionary changes that prevent *virosk* from specifying germ plasm in a *D. melanogaster* background.

Methods

Annotated *oskar* orthologs from *D. melanogaster* [GenBank NM_169248.1; FlyBase CG10901-PA], *Drosophila simulans* [GenBank XM_002104160.1; FlyBase GD18580-PA], *Drosophila sechellia* [GenBank XM_002031933.1; FlyBase GM23770-PA], *Drosophila yakuba* [GenBank XM_002096839.1; FlyBase GE25914-PA], *Drosophila erecta* [GenBank XM_001980858.1; FlyBase GG13545-PA], *Drosophila ananassae* [GenBank XM_001953262.1; FlyBase GF17692-PA], *Drosophila pseudoobscura* [GenBank XM_001359471.2; FlyBase GA10627], *Drosophila persimilis* [GenBank XM_002017349.1; FlyBase GL21554-PA], *Drosophila willistoni* [GenBank XM_002070244.1; FlyBase GK11117-PA], and *D. virilis* [GenBank XM_002053233.1; FlyBase GJ23790-PA] were obtained from FlyBase (www.flybase.org). Coding sequence of *D. immigrans oskar* was obtained from GenBank [DQ823084.1]. We also identified *oskar* orthologs from the following recently sequenced species whose genomes have not been annotated: *Drosophila eugracilis* [genomic scaffold: GenBank JH402624.1], *Drosophila ficusphila* [genomic scaffold: GenBank GL987928.1], *Drosophila biarmipes* [genomic scaffold: GenBank JH400370.1], *Drosophila takahashii* [genomic scaffold: GenBank JH112313.1], *Drosophila elegans* [genomic scaffold: GenBank JH110107.1], *Drosophila rhopaloa* [genomic scaffold: GenBank JH406433.1], *Drosophila kikkawai* [genomic scaffold: GenBank JH111367.1], *Drosophila bipectinata* [genomic scaffold: GenBank JH401929.1]. Genome sequences for these species were accessed via the Drosophila Species Stock Center at https://stockcenter.ucsd.edu/info/welcome.php. We conducted a tBLASTn search of each Drosophilid genome with *D. melanogaster* Oskar protein as the query to uncover the most similar coding sequence with respect to amino acid conservation. As *oskar* is a single-copy gene in all genomes examined to date, and shares no significant overall sequence similarity with non-*oskar* genes (Lynch et al. 2011), the top tBLASTn hit was considered to be the ortholog. To extract the coding sequence from genomic scaffold sequences we used the Augustus gene predictor (Keller et al. 2011), and manually curated the resulting sequences to mask stop codons and frame shift mutations. Reciprocal BLAST of the top predicted coding sequences to *D. melanogaster* was performed to confirm orthology. Nucleotide sequences of all *oskar* orthologs analysed in this study are provided in Online Resource 1.

As the results of PAML analyses can be sensitive to the alignment methods used (Blackburne and Whelan 2013), we generated multiple sequence alignments using two different methods, and performed analyses on the results of both MSAs. The sequences of the 18 *Drosophila* species were multiply aligned using MUSCLE implemented in TranslatorX (Abascal et al. 2010), or using PRANK (Löytynoja and Goldman 2008). We did not include the *D. willistoni* sequence as its predicted length was less than 60 % that of *D. melanogaster oskar* (not shown). There is no evidence for unusual divergence of *D. willistoni oskar*; this is therefore likely due to sequencing or annotation error.

Predicted structural and interaction domains were manually extracted from the whole gene alignment using the known acid residues corresponding to each domain in *D. melanogaster* (Fig. 1) (Breitwieser et al. 1996; Suyama et al. 2009; Anne 2010). Sequences from Valois-interacting regions were concatenated for analysis. The PRANK alignment was subjected to GBlocks analysis using the default options (minimum number of sequences for a conserved position: 10; minimum number of sequences for a flanking position: 10; maximum number of contiguous positions: 8; minimum length of a block: 5).

We repeated the branch site test for domains that showed a consistent signature for positive selection using the reported cDNA sequence of *D. virilis oskar* (Genbank_L22556.1) that was used in the experiments that suggested functional divergence of *D. virilis* and *D. melanogaster oskar* with respect to germ plasm assembly (Webster et al. 1994) (Online Resource 1). We also used Sanger sequencing to confirm the entire nucleotide sequence of this *D. virilis* allele (see Online Resource 1).

Results and Discussion

The complete *oskar* coding region is under purifying selection

We obtained *oskar* coding sequences from the Drosophilid genome sequences, as well as the sequenced *D. immigrans oskar* coding region (Fig. 2; Online Resource 1), and generated multiple sequence alignments using two different multiple sequence alignment (MSA) tools, the similarity-based MSA MUSCLE (Edgar 2004) (Online Resource 2, Figure S1) and the evolutionarily informed MSA PRANK (Löytynoja and Goldman 2008) (Online Resource 3, Fig S2). Because the choice of MSA can influence the outcome of such analyses (Blackburne and Whelan 2013), we performed evolutionary rate analyses using both MSA outputs. We conducted maximum likelihood analyses with codeml implemented in PAML v4 (Yang 2007) to estimate non-synonymous (d*N*) and synonymous (d*S*) substitution

rates, and their ratio (ω=d*N*/d*S*). We then used the Likelihood Ratio Test to compare the fit of different evolutionary models to the data (Yang 2007; Yang et al. 2000b).

We first applied the simplest model M0, which sets all branches and sites to evolve at the same rate, to obtain a single global ω estimate for the entire *oskar* coding region alignment (Yang et al. 2000a). The log likelihood for this model was −4,397.07 using the MUSCLE alignment, and −16,563.12 using the PRANK alignment, with ω estimates of 0.32 and 0.16, respectively, indicating overall purifying selection of full-length *oskar*.

Distinct *oskar* domains are evolving at different rates

Next, to estimate ω for each domain separately and test if these domains were under different selective constraints, we applied different fixed site models (Yang and Swanson 2002). The highest log likelihood was obtained using model E (MG4), which assumes different ω, κ (transition/transversion ratio), π (equilibrium codon frequencies), and *r*s (proportional branch lengths) between *oskar* domains. Using either the MUSCLE MSA (Online Resource 2, Table S1) or the PRANK MSA (Online Resource 3, Table S4), the fit of this model was significantly better than that of model B, which assumes identical κ, ω, and π but different *r*s (P<0.001). This shows that the strength of selection varies among distinct *oskar* domains. Estimates of ω were less than 1 for all domains, indicating overall purifying selection on each domain (Fig. 1b). However, the SGNH, LOTUS, and Valois-interacting domains are the most constrained, while the Lasp-binding and Long Osk domains are evolving approximately four to five and two to three times faster, respectively, than the former three domains. This suggests that evolutionary changes in *oskar* function may not be due to changes within the SGNH, LOTUS, or Valois-interacting domains. Moreover, it is consistent with the relatively poor conservation of the Lasp-binding region across insects (Lynch et al. 2011) and the recent evolution of Long Osk in the *Drosophila* lineage. As selective pressures on individual *oskar* domains are heterogeneous, further analyses were conducted separately for each domain.

Evidence for positive selection on specific *oskar* domains

Given the functional divergence of *Drosophila oskar*, we asked whether positive selection might be acting on specific amino acids of any Oskar domain. To test this hypothesis, we applied different site models that set the ω ratio to vary among sites (Yang et al. 2000a, 2005). Comparison of models M1 (nearly neutral; assumes two site classes in the sequence with ω_0<1 and ω_1=1) and model M2 (adds site class ω_2 allowing for positive selection) was not significant for any domain using either of the MUSCLE (Online Resource 2, Table S2) or PRANK (Online Resource 3, Table S5) alignments (Table 1). Comparison of models M7 (assumes a beta distribution of ω over sites) and M8 (adds an extra site class with a free ω ratio estimated from the data, allowing ω values greater than 1) also showed no significant differences for any single domain for either of the MUSCLE or PRANK alignments (Table 1).

The results of the analyses thus far show that when using site models to consider the evolution of Oskar orthologs from these 18 *Drosophila* lineages, no specific domain appears to be under positive selection. However, if a gene evolves under purifying selection most of the time, but is occasionally subject to episodes of adaptive change, site models may not yield a significant d*N*/d*S* value. Given the inability of *D. virilis oskar* to substitute for *D. melanogaster oskar*, we wished to test the hypothesis that positive selection might be acting on the *D. virilis* branch alone. We therefore assessed differences in ω on that specific branch using branch site models (Zhang et al. 2005). We used the modified model A, or test 2, because it is more conservative, yields fewer false positives, and is better able to distinguish relaxed selective constraint from positive selection (Zhang et al. 2005). Setting the *D. virilis* branch as the foreground branch, we tested whether model MA (which assumes three site classes, $0>\omega_0<1$ between 0 and 1, and $\omega_1=1$ and $\omega_2>1$ only for the foreground branch) fit the data better than the alternative model MA_{fix} (which fixes ω_2 at 1 in foreground branches). Using either of the MUSCLE (Online Resource 2, Table S3) or PRANK (Online Resource 3, Table S6) alignments, we found that comparisons between MA and MA_{fix} were not significant for the LOTUS or SGNH predicted structural domains, or for the Valois interaction domain (Table 1). Under the MUSCLE MSA analysis of the Lasp-binding domain, the log likelihood of the MA model (−2,350.39) was greater than that of the MA_{fix} model (−2,352.01) (χ^2=3.24, P=0.07) (Table 1; Online Resource 2, Table S3), but the difference was not significant. We note here that PAML documentation recommends the use of a critical value of χ^2 (3.84 at 5 % and 5.99 at 1 %) to guide against violation of model assumptions for branch site models (Yang 2007.

In contrast, the PRANK MSA analysis did reveal a statistically significant signature of positive selection for the Lasp-binding domain (χ^2=7.9; P<0.01) on the *D. virilis* branch (Table 1; Online Resource 3, Table S6). The PRANK MSA analysis also identified significant signatures of positive selection for the Vasa-interacting domain (χ^2=5.1; P<0.05) (Table 1; Online Resource 3, Table S6). This suggests some residues within these domains could be evolving under positive selection and may contribute to *oskar* functional evolution. Strikingly, we found that under both the MUSCLE (χ^2=14.7; P<0.001) and PRANK (χ^2=5.43; P<0.05) MSA analyses, the MA

Table 1 Likelihood Ratio Test statistics for Oskar predicted structural and interaction domains: 18 species analyses

	MUSCLE MSA			PRANK MSA		
	M1 vs M2[1]	M7 vs M8	MA vs MA_{fix}	M1 vs M2[1]	M7 vs M8	MA vs MA_{fix}
Long Osk	0 (1.0000)	0 (1.0000)	14.7 (0.0001)***	0 (1.0000)	1.47 (0.4795)	5.43 (0.0198)*
LOTUS	0 (1.0000)	1.44 (0.4858)	1.05 (0.3055)	0 (1.0000)	0.08 (0.9608)	1.05 (0.3055)
Lasp-binding	0.04 (0.9802)	2.91 (0.2334)	3.24 (0.0719)	0.09 (0.9560)	3.71 (0.1565)	7.9 (0.0049)**
SGNH Hydrolase	0 (1.0000)	5.73 (0.0561)	0 (1.0000)	0 (1.0000)	5.94 (0.0515)	0 (1.0000)
Vasa-interacting	0 (1.0000)	0.35 (0.8395)	0.66 (0.4166)	0 (1.0000)	3.24 (0.1979)	5.1 (0.0239)*
Valois-interacting	0 (1.0000)	3.72 (0.1557)	0 (1.0000)	0 (1.0000)	4.57 (0.1080)	0 (1.0000)

Values in each column correspond to twice the difference of log likelihood of the two nested models, with *P* values indicated in parentheses

*$P<0.05$; **$P<0.01$; ***$P<0.0001$

model fit the data significantly better than MA_{fix} for the Long Osk domain (Table 1), suggesting that non-synonymous changes at some Long Osk codons may additionally have been subject to positive selection on the *D. virilis* branch.

While the branch site analyses indicate positive selection for Long Osk and Lasp-binding domains, they may be affected by the large divergence time between *D. immigrans*, *D. virilis*, and *D. melanogaster*, the three species for which functional data are available. Highly divergent sequences could suffer from alignment errors, which can lead to false positives with the branch site model (Markova-Raina and Petrov 2011; Anisimova and Yang 2007). Removing unreliable alignment regions is expected to increase the accuracy of positive selection inference, although such filtering may also significantly decrease the power of the test, as positively selected regions are fast evolving, and those same regions are often those that are most difficult to align (Privman et al. 2012). In order to gain insight into whether Oskar sequence divergence across the 18 Drosophilids may have affected our inference of positive selection, we repeated the branch site test for positive selection on the Lasp-binding, Long Osk and Vasa-interacting domain using a new set of edited alignments, that we call here "conserved sequence block" alignments. To make these alignments, we removed poorly aligned sites in the original full-length Oskar PRANK alignment using Gblocks (Castresana 2000) and then conducted the branch site test analysis on the remaining conserved sequence blocks of each domain (Online Resource 4, Figure S3). Even with this conservative approach, we continued to see a significant signature for positive selection on the *D. virilis* branch for both the Lasp-binding ($\chi^2=4.21$; $P<0.05$) and Long Osk domains ($\chi^2=4.76$; $P<0.05$) (Table 2; Online Resource 4, Table S7). Comparisons between MA and MA_{fix} were not significant for the Vasa-interacting region ($P=0.34$) (Online Resource 4, Table S7). Thus, even with a conservative approach the Long Osk and Lasp-binding domains are indicated as being under positive selection on the *D. virilis* branch in our analysis of 18 *Drosophila* species.

Candidate sites for functional divergence between *D. virilis* and *D. melanogaster oskar*

To identify candidates for specific sites that could be evolving under positive selection in our 18 species analysis, we applied the Bayes Empirical Bayes (BEB) approach to all alignments that showed a statistically significant signature for adaptive evolution on the *D. virilis* branch, namely (1) the MUSCLE alignment of the Long Osk domain extracted from the original alignment of full-length Oskar (Online Resource 2, Figure S1); (2) PRANK alignments of the entire Long Osk, Lasp-binding, and Vasa-interacting domains extracted from the original alignment of full-length Oskar (Online Resource 3, Figure S2); and (3) the conserved sequence blocks of the Long Osk and Lasp-binding domains obtained by trimming poorly aligned regions from the original full-length PRANK MSA alignment (Online Resource 4, Figure S3). To be conservative we focused only on sites with a BEB posterior probability of being under positive selection greater than 0.9.

Table 2 Likelihood ratio test statistics for MA vs MA_{fix} model for Long Osk, Lasp-binding and Vasa-interacting domains aligned with PRANK MSA

	Conserved sequence blocks	Seven species alignment
Long Osk	4.76 (0.0291)*	0 (1.0000)
Lasp-binding	4.21 (0.0402)*	0 (1.0000)
Vasa-interacting	0.92 (0.3375)	0.43 (0.5120)

Values in each column correspond to twice the difference of log likelihood of the two nested models, with *P* values indicated in parentheses

*$P<0.05$

Using these criteria, we identified five residues, two in the Long Osk domain and three in the Lasp-binding domain that may be evolving under positive selection on the *D. virilis* branch.

Analysis of the Long Osk domain extracted from the MUSCLE MSA of full-length Oskar identified one residue with signatures of positive selection (*D. melanogaster* F51 (residue numbers throughout refer to the position in the primary amino acid sequence of *D. melanogaster* Long Oskar); Online Resource 2, Figure S1). In addition, analyses of the Long Osk domain extracted from the PRANK alignment of full-length Oskar, and of the conserved sequence blocks of Oskar, both supported the hypothesis of positive selection at a second residue (*D. melanogaster* R65; Online Resource 3, Figure S2; Online Resource 4, Figure S3).

In the Lasp-binding domain, analysis of this domain extracted from the PRANK MSA of full-length Oskar (Online Resource 3, Figure S2) identified two residues (*D. melanogaster* E306 and P353) as being under positive selection. These two residues were also identified as being under positive selection by analysis of the Vasa-interaction domain extracted from the full-length PRANK MSA (Online Resource 3). Finally, a third residue (*D. melanogaster* Y339) was identified by analysis of the Lasp-binding domain derived from the conserved sequence block PRANK MSA (Online Resource 4, Figure S3).

If changes of amino acid identity at these sites contributed to the functional divergence between *D. melanogaster* and *D. virilis* Oskar, we might expect these residues to have different physicochemical characteristics in the two species. Consistent with this idea, we found that at three of the five candidate sites, one in the Long Osk domain and two in the Lasp-binding domain, amino acid differences between *D. virilis* and *D. melanogaster* result in changes in one or both of polarity and acid–base properties (Table 3, Fig. 3). This supports the hypothesis that changes at these residues may be linked to the functional divergence between *D. melanogaster* and *D. virilis* Oskar, making these residues promising candidates for future functional verification in vivo.

Analysis of *D. melanogaster* subgroup species

A second issue related to the high divergence time between our species of interest is that the saturation of d*S* in highly divergent sequences is expected to inflate false positive rates of likelihood ratio tests for positive selection (Gharib and Robinson-Rechavi 2013). Determining the optimal analytical

Table 3 Chemical properties of amino acids under positive selection in the branch leading to *D. virilis*

PP value of positive selection	AA position in *D. melanogaster*[a]	*D. virilis* AA				*D. melanogaster* AA				Polarity change	Acidity change
		AA	Polarity	pH	Hydro	AA	Polarity	pH	Hydro		
Long Oskar domain—MUSCLE MSA (supported by full-length genomic and Macdonald allele)											
0.99[b]	*51*	*K*	*Polar*	*Basic*	*Philic*	*F*	*Nonpolar*		*Phobic*	*Y*	*Y*
Long Oskar domain—PRANK MSA (supported by analysis of full-length and conserved sequence blocks alignments of genomic allele and full-length Macdonald allele)											
0.92/0.91/0.95[c]	65	R	Polar	Basic	Philic	R	Polar	Basic	Philic	N	N
Lasp-binding domain—PRANK MSA (supported by full-length alignment)											
0.99[d]	353	A	Nonpolar		Phobic	P	Nonpolar		Phobic	N	N
0.98/0.95[e]	*306*	*M*	*Nonpolar*		*Phobic*	*E*	*Polar*	*Acidic*	*Philic*	*Y*	*Y*
Lasp-binding domain—PRANK MSA (supported by genomic allele conserved sequence blocks alignment and full-length Macdonald allele)											
0.95/0.98[f]	*339*	*H*	*Polar*	*Basic*	*Philic*	*Y*	*Polar*		*Philic*	*N*	*Y*

[a] Amino acid position refers to the *D. melanogaster* residue position in the unaligned primary amino acid sequence

[b] Rows in italics indicate residues under positive selection that have different chemical properties between *D. virilis* and *D. melanogaster*. The BEB posterior probability values from MUSCLE MSA alignment analyses using the genomic *D. virilis* allele or the Macdonald allele were the same for both alignments (see Online Resources 2, 8)

[c] Indicates the posterior probability values from three different PRANK MSA analyses for one of two residues in the Long Oskar domain identified as being under positive selection. BEB values are from analysis of full-length Oskar alignment and conserved sequence blocks alignment with genomic *D. virilis* allele, and full-length alignment generated using *D. virilis* Macdonald allele, respectively (see Online Resources 3, 4, 9)

[d] This residue differs between the genomic and Macdonald alleles, and shows signatures of positive selection only under the analysis of a PRANK alignment using the genomic allele, but not the Macdonald allele (see Online Resources 3, 7)

[e] Indicates the posterior probability values from two different PRANK MSA analyses for the first of three residues in the Lasp-binding domain identified as being under positive selection. BEB values are from analysis of full-length Oskar alignments generated with the genomic and Macdonald *D. virilis* alleles, respectively (see Online Resources 3, 9)

[f] Indicates the posterior probability values for the second of three residues in the Lasp-binding domain identified by two different PRANK MSA analyses as being under positive selection (see Online Resources 4, 9). BEB values are from analysis of conserved sequence blocks alignment and full-length alignment generated using *D. virilis* allele from Webster et al (1994), respectively

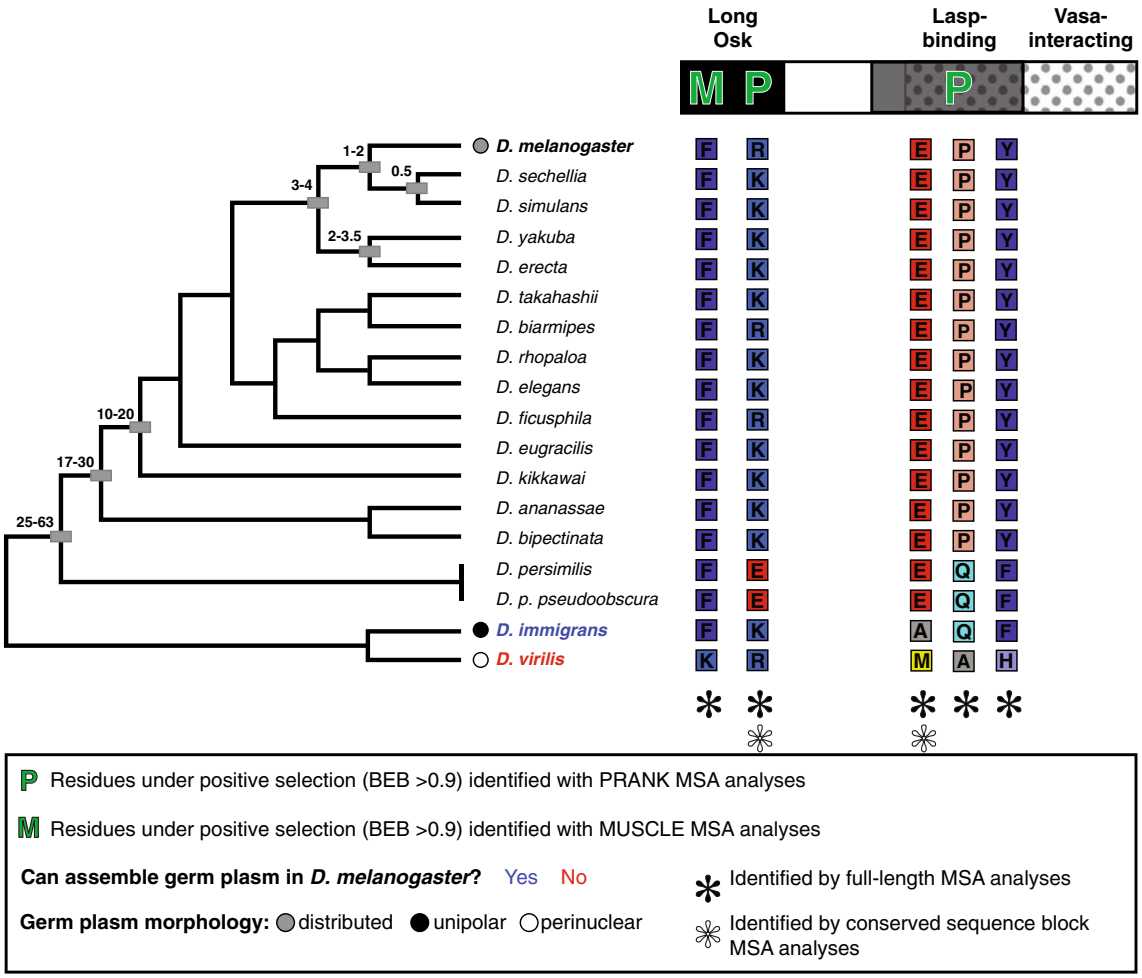

Fig. 3 Phylogenetic relationships and physicochemical properties of positively selected *oskar* residues of 18 *Drosophila* species. *Left* side shows phylogenetic relationships between the 18 species whose *oskar* sequences were analyzed in this study. Species names in colored text (*red*/*blue*) in tree at left indicate functional conservation of *oskar* with respect to potential for germ plasm assembly in *D. melanogaster* (Webster et al. 1994; Jones and Macdonald 2007). *Shaded circles* indicate germ plasm morphology as determined by histology and electron microscopy (*black* unipolar; *gray* distributed; *white* perinuclear; see Additional File 12 for details) (Counce 1963; Mahowald 1968). Among the species shown, functional data on *oskar's* germ plasm assembly capabilities in *D. melanogaster*, and morphological data on germ plasm morphology, are only currently available for *D. melanogaster, D. immigrans* and *D. virilis*. Phylogenetic relationships according to topology used for PAML analysis (Fig. 2), which is consistent with current hypotheses (Yang et al. 2012; Kopp 2006). Numbers at selected nodes indicated estimated divergence times in Mya; estimates from (Obbard et al. 2012; Remsen and O'Grady 2002). *Right side* shows amino acid identities of those Oskar residues that appeared positively selected in the branch leading to *D. virilis* by each of the analyses performed with two different MSA, MUSCLE (in the Long Osk domain; leftmost residue) and PRANK (one in the Long Osk domain and three in the Lasp-binding and Vasa-interacting domains; remaining four residues). Residues are shown in the N-terminal to C-terminal order in which they appear in the indicated protein domains, colored according to the RasMol amino acid color scheme (Sayle and Milner-White 1995) (see Table 3 for details)

design for these studies is challenged, however, by the fact that the phylogenetic boundaries for points of saturation, and the extent to which the branch site test is affected by divergence time, are not clear (Gharib and Robinson-Rechavi 2013). Nonetheless, we undertook two additional analyses as a further step towards gaining some insight into the effect of divergence on our inferences of positive selection.

First, we assessed the relative rates of evolution of predicted structural and functional domains using a reduced set of sequences with relatively low divergence. We generated MUSCLE alignments of the five species of the *D. melanogaster* subgroup (Online Resource 5, Figure S4), which are often considered to be at an appropriate level of divergence for PAML analyses (Clark et al. 2007; Larracuente et al. 2008), as they diverged from a last common ancestor only approximately 3–4 Mya (Tamura et al. 2004). Analyses of only these sequences should thus avoid the potential problem of saturation of d*S*. The global rate of evolution of *oskar* in these five species using model MO was 0.25 with a log likelihood of −4,086.41, indicating overall purifying selection as observed in the analysis of 18 species. Next, we used this alignment to assess rates of evolution of the component subdomain models using the MG4

model, and again obtained the same results as those obtained with the alignment containing 18 species (Fig. 1b). ω values for each domain showed that SGNH was the most conserved domain, while the Long Osk and Lasp-binding domains were the two most rapidly evolving (Online Resource 5, Table S8). However, in contrast to our original 18 species analysis, neither partition nor site tests detected significant positive selection for any domain except LOTUS, which was significant with P=0.04 (Online Resource 5, Table S9, Table S10).

Second, to test for positive selection on the *D. virilis* branch, we generated another set of PRANK alignments using a subset of sequenced *Drosophila* species comprising those in *D. melanogaster* subgroup, plus *D. immigrans* and *D. virilis*, the only two non-*melanogaster* species for which data on *oskar* function are available (Webster et al. 1994; Jones and Macdonald 2007) (Online Resource 6, Figure S5). These alignments, like those of the *melanogaster* subgroup sequences, should be less likely than the full 18 species analysis to suffer from problems with saturated synonymous sites and inaccurate alignments. We used these seven species alignments to assess rates of evolution of the component subdomain using the MG4 model, and obtained the same results as those obtained with the alignment containing 18 species (Fig. 1b). ω values for each domain showed that SGNH was the most conserved domain, while the Long Osk and Lasp-binding domains were the two most rapidly evolving (Online Resource 6, Table S11). However, branch site test comparison of MA with MA_{fix} was not significant for any of the Lasp-binding (χ^2=0; P=1), Long Osk (χ^2=0; P=1) or Vasa-interacting domains (P=0.51) (Table 2; Online Resource 6, Table S12).

Assessment of putative polymorphisms in *D. virilis oskar*

All analyses described above used the *oskar* nucleotide sequence annotated from the *D. virilis* genome (Clark et al. 2007) (NCBI accession XM_002053233.1; henceforth designated "genomic allele"). However, we noticed that the translation of this sequence differs from the reported *D. virilis oskar* cDNA translation (Webster et al. 1994) (NCBI accession L22556.1; henceforth designated "Macdonald allele") by two amino acids in the Long Osk region (QQ66-67 indel), and three amino acids in the Lasp-binding region (A341P, H348 indel, P383R) (Online Resource 7, Figure S6). We used Sanger sequencing to confirm that the sequence of the Macdonald allele was identical to that reported in NCBI accession L22556.1, except for one residue (A341P) that matched the genomic allele rather than the Macdonald allele (Online Resource 7). Because the Macdonald allele was used for the transgenic experiments that suggested functional divergence between *D. virilis* and *D. melanogaster oskar* (Webster et al. 1994), we repeated the branch site test for 18 species using the Macdonald allele sequence, and focused our analysis on those protein domains and residues that showed a consistent signal for positive selection. Specifically, these were the Long Oskar domain aligned with the MUSCLE MSA, and the Long Oskar and Lasp-binding domains aligned with the PRANK MSA. We found that the same domains and residues were predicted to be under positive selection regardless of whether we used the genomic or Macdonald alleles for analysis. Specifically, we found a significant signal of positive selection on the Long Osk domain using the MUSCLE alignment of the Macdonald allele (χ^2=8.44; P=0.0037) (Online Resource 8, Table S13). Within the Long Osk domain, the same residue (*D. melanogaster* F51) was identified as being under positive selection in analyses of both alleles. Similarly, we found a significant signal of positive selection on the Long Osk domain using the PRANK alignment of the Macdonald allele (χ^2=5.76; P=0.016) (Online Resource 9, Table S14), and within this domain, the same residue (*D. melanogaster* R65) was identified as being under positive selection in analyses of both alleles. We also detected a significant signature of positive selection for the Lasp-binding region (χ^2=5.5; P=0.019) on the *D. virilis* branch using the PRANK alignment and the Macdonald allele. This analysis identified two residues: *D. melanogaster* E306, which was also identified in the analysis of the full-length PRANK alignment of the genomic allele (Online Resource 3), and *D. melanogaster* Y339, which was also identified in the PRANK analysis of conserved sequence blocks of the genomic allele (Online Resource 4).

Thus, the minor sequence differences between the Macdonald and genomic alleles do not change our detection of signatures of positive selection on the same domains and residues of Oskar. The specific residues thus identified differ as a function of the alignment method used, but not due to the *D. virilis oskar* sequence used. The only exception is a single residue, *D. melanogaster* P353, which was identified as being under positive selection in the PRANK analysis of the genomic allele but not of the Macdonald allele. This is likely due to the fact that this residue is different in the Macdonald allele (A341P). We therefore cannot conclude that this particular residue is a candidate for functional divergence between the two species. Overall, we conclude that while there are a small number of polymorphisms in sequenced *D. virilis oskar* alleles, our results are generally robust to these minor sequence differences.

In summary, all analyses clearly support heterogeneous rates of evolution on distinct Oskar domains, with Long Osk and Lasp-binding being the fastest evolving. However, we cannot exclude the possibility that signatures of positive selection on these domains, which were detected only with the 18 species analyses, may be false positives. Alternatively, the lack of a significant signal for positive selection in the seven species analysis could be due to the decrease in power that results from using fewer sequences. In support of the positive selection result obtained with the 18 species analyses,

simulations have shown that the branch site model is more robust to high sequence divergence than might have been expected (Gharib and Robinson-Rechavi 2013; Studer et al. 2008), and that high d*S* values may be more of a concern for false negatives than false positives (Gharib and Robinson-Rechavi 2013).

Overall, the effects of sequence divergence and d*S* saturation are complex and difficult to fully resolve. Nonetheless, the consistent pattern of higher rates of evolution of Long Osk and Lasp-binding domains seen in all analyses of five species, seven species and 18 species alignments make changes in these domains strong candidates for functional divergence between *Drosophila* Oskar proteins. We further suggest that the specific sites within these domains exhibiting changes in physicochemical properties between *D. virilis* and *D. melanogaster* are strong candidates for changes underlying the functional divergence of Oskar between *D. melanogaster* and *D. virilis*. However, we note that caution is warranted in the inference of positive selection on these sites along the *D. virilis* branch.

The roles of *oskar* in the evolution of germ plasm morphology

To date the functional characteristics of *oskar* with respect to germ plasm assembly have been tested for the orthologs of only three *Drosophila* species: *D. melanogaster*, *D. immigrans* (*immosk*), and *D. virilis* (*virosk*). All of these species possess germ plasm, but the germ plasm morphology is distinct in each species (Mahowald 1962, 1968; Counce 1963). Mapping germ plasm morphology on to a phylogeny of Drosophilids (Online Resource 10) shows that germ plasm morphology displays some clade-specific patterns. We hypothesize that changes in germ plasm morphology may be the result of evolutionary changes in *oskar* function. In support of this hypothesis, as noted above *immosk* can assemble a functional germ plasm that has a *D. immigrans* morphology in a *D. melanogaster* context (Jones and Macdonald 2007). In contrast, *virosk* cannot assemble functional germ plasm in a *D. melanogaster* context (Webster et al. 1994). This indicates that the characteristics of germ plasm morphology and the assembly of germ plasm itself are both processes directed by *oskar*. At present, *oskar* orthologs have not been identified for most species with well-studied germ plasm morphology (Online Resource 10), and germ plasm morphology has not been characterized for most of the species whose *oskar* sequence has been determined. Further studies that fill these knowledge gaps will be useful in determining the specific changes in *oskar* that accompanied and/or led to evolutionary changes in germ plasm morphology and function within Drosophilids.

Possible significance of the evolution of the *Drosophila*-specific Long Oskar domain

The Long Oskar domain was identified by both MUSCLE and PRANK MSA analyses as possibly being under positive selection in the lineage leading to *D. virilis*. Known *oskar* loss of function alleles in *D. melanogaster* do not contain lesions in the Long Oskar domain, and therefore do not shed light on the potential functions of the positively selected amino acids identified in this study. However, evidence from studies of *D. melanogaster* suggests that this domain may play a role in stabilizing assembled germ plasm. During oogenesis, *osk* mRNA is synthesized and transported to the posterior pole of the oocyte (Rongo et al. 1995), where it is translated into the Long Osk and Short Osk isoforms from two alternative start codons (Markussen et al. 1995). The Long Osk isoform includes all four protein domains described above, whereas the Short Osk isoform excludes the Long Oskar domain and thus consists only of the LOTUS, Lasp-binding and SGNH domains. The two isoforms exhibit distinct molecular affinities for germ plasm components (Breitwieser et al. 1996; Suyama et al. 2009; Babu et al. 2004) and localize to distinct subcellular compartments (Vanzo et al. 2007), but both are required for effective germ plasm assembly. Short Osk alone is able to assemble enough germ plasm to yield a low frequency of germ cell formation (Markussen et al. 1995), but cannot efficiently maintain *oskar* mRNA or protein at the posterior pole (Vanzo and Ephrussi 2002). In contrast, Long Osk can maintain both *oskar* mRNA and Oskar protein at the posterior pole, but no germ cells form when only Long Osk is expressed, suggesting that it cannot efficiently assemble stable germ plasm. The current model for Osk-mediated germ plasm assembly in *D. melanogaster* is thus one in which Long Osk anchors Short Osk to the posterior oocyte cortex, and Short Osk in turn localizes multiple germ cell determinants. The fact that *Nasonia vitripennis* (Hymenoptera) *oskar* lacks the Long Osk domain but nonetheless appears to act as a functional germ plasm determinant (Lynch et al. 2011), raises the question of what the functional significance of the evolution of the Long Osk domain might be.

One possibility is that the evolution of the Long Oskar domain was linked to the emergence of additional mRNA localization mechanisms that increased the stability of *oskar* mRNA at the oocyte posterior. This could have been beneficial in improving the stability of germ plasm and increasing robustness of *oskar*-directed germ cell specification. Consistent with this hypothesis, although *oskar* mRNA is localized to embryonic germ plasm in all studied holometabolous insects, its localization to the oocyte posterior cortical cytoplasm prior to germ cell formation is variable, and correlates with the presence or absence of the Long Oskar domain. In *D. melanogaster*, *oskar* mRNA (as visualized by in situ hybridization) is very tightly localized in a thin crescent

(Ephrussi et al. 1991), but in *D. virilis*, comparable gene expression methods show that only some *oskar* mRNA is localized to a small spot at the posterior cortex, while additional transcripts are localized in a diffuse cloud in an apparent posterior to anterior gradient (Webster et al. 1994). In holometabolous insects without a Long Osk isoform (the wasp *Nasonia vitripennnis*, the ant *Messor pergandi* (Lynch et al. 2011), and the mosquitoes *Aedes aegypti* (Juhn and James 2006) and *Culex quinquefasciatus* (Juhn et al. 2008)), posterior *oskar* mRNA localization also appears more diffuse than in *D. melanogaster*. Finally, the only *oskar* ortholog identified to date in a hemimetabolous insect (the cricket *Gryllus bimaculatus*) also lacks a Long Oskar domain, and its mRNA is distributed ubiquitously in oocytes and embryos, showing no asymmetric localization at all (Ewen-Campen et al. 2012).

Conclusions

While *D. melanogaster oskar* function has been well characterized at the genetic level, the specific molecular mechanisms by which it functions remain unknown. Previous comparative approaches using the entire gene have shown functional divergence of *Drosophila oskar* (Jones and Macdonald 2007; Webster et al. 1994) but have not identified the specific regions or selective pressures involved. Our molecular evolution analysis shows that the two fastest evolving domains, Long Osk and Lasp-binding, also show a statistically significant signature of positive selection on the *D. virilis* branch in our analysis of 18 species orthologs. Specific putatively positively selected sites within these domains also exhibit major differences in the physicochemical properties of amino acids between *D. melanogaster* and *D virilis*. However, the high divergence time between *D. melanogaster*, *D. immigrans*, and *D. virilis* means that we can only cautiously infer positive selection at these sites. Further polymorphism-based tests of positive selection will be required to elucidate the selection pressures involved. Nonetheless, based on their faster rate of evolution, we suggest that changes in the Long Oskar and Lasp-binding domains underlie functional differences between the Oskar proteins. Functional verification of the roles of these domains and specific sites will be required to evaluate the contributions of each of these candidates to the evolution of *oskar* function. The Long Osk and Lasp-binding domains are the first candidates for *oskar* functional evolution identified using an evolutionary approach, and provide specific hypotheses that can be tested for functional verification in future in vivo studies. This analysis thus represents an important step towards understanding the role of Oskar in germ plasm evolution and assembly.

Acknowledgments Thanks to Paul Macdonald for the plasmid containing the *D. virilis* oskar cDNA, to John Srouji for Sanger sequencing and discussion of the results, to Victor Zeng and Amit Indap for assistance with preliminary analyses, and to Extavour lab members for discussion of the manuscript. This work was partly supported by NSF grant IOS-0817678 to CGE and funds from Harvard University.

Competing interests The authors declare that they have no competing interests.

Author contributions AA conceived of the study, created alignments, and performed evolutionary rate analyses. CGE assisted with study design and performed analyses of amino acid physicochemical properties and phylogenetic distribution of germ plasm morphology. Both authors wrote and approved the final manuscript.

References

Abascal F, Zardoya R, Telford MJ (2010) TranslatorX: multiple alignment of nucleotide sequences guided by amino acid translations. Nucleic Acids Res. doi:10.1093/nar/gkq291, 38 (Web Server issue): W7-13

Anantharaman V, Zhang D, Aravind L (2010) OST-HTH: a novel predicted RNA-binding domain. Biol Direct 5:13. doi:10.1186/1745-6150-5-13

Anisimova M, Yang Z (2007) Multiple hypothesis testing to detect lineages under positive selection that affects only a few sites. Mol Biol Evol 24(5):1219–1228. doi:10.1093/molbev/msm042

Anne J (2010) Targeting and anchoring Tudor in the pole plasm of the *Drosophila* Oocyte. PLoS ONE 5(12):e14362. doi:10.1371/journal.pone.0014362

Babu K, Cai Y, Bahri S, Yang X, Chia W (2004) Roles of Bifocal, Homer, and F-actin in anchoring Oskar to the posterior cortex of *Drosophila* oocytes. Genes Dev 18(2):138–143. doi:10.1101/gad.282604

Blackburne BP, Whelan S (2013) Class of multiple sequence alignment algorithm affects genomic analysis. Mol Biol Evol 30(3):642–653. doi:10.1093/molbev/mss256

Blackstone NW, Jasker BD (2003) Phylogenetic considerations of clonality, coloniality, and, mode of germline development in animals. J Exp Zool B Mol Dev Evol 297B(1):35–47

Breitwieser W, Markussen F-H, Horstmann H, Ephrussi A (1996) Oskar protein interaction with Vasa represents an essential step in polar granule assembly. Genes Dev 10:2179–2188

Callebaut I, Mornon J-P (2010) LOTUS, a new domain associated with small RNA pathways in the germline. Bioinformatics 26(9):1140–1144. doi:10.1093/bioinformatics/btq122

Castresana J (2000) Selection of conserved blocks from multiple alignments for their use in phylogenetic analysis. Mol Biol Evol 17(4): 540–552

Cavey M, Hijal S, Zhang X, Suter B (2005) *Drosophila valois* encodes a divergent WD protein that is required for Vasa localization and Oskar protein accumulation. Development 132(3):459–468

Clark AG, Eisen MB, Smith DR, Bergman CM, Oliver B, Markow TA, Kaufman TC, Kellis M, Gelbart W, Iyer VN, Pollard DA, Sackton TB, Larracuente AM, Singh ND, Abad JP, Abt DN, Adryan B, Aguade M, Akashi H, Anderson WW, Aquadro CF, Ardell DH, Arguello R, Artieri CG, Barbash DA, Barker D, Barsanti P, Batterham P, Batzoglou S, Begun D, Bhutkar A, Blanco E, Bosak SA, Bradley RK, Brand AD, Brent MR, Brooks AN, Brown RH, Butlin RK, Caggese C, Calvi BR, Bernardo de Carvalho A, Caspi A, Castrezana S, Celniker SE, Chang JL, Chapple C, Chatterji S, Chinwalla A, Civetta A, Clifton SW, Comeron JM, Costello JC, Coyne JA, Daub J, David RG, Delcher AL, Delehaunty K, Do CB, Ebling H, Edwards K, Eickbush T, Evans JD, Filipski A, Findeiss S,

Freyhult E, Fulton L, Fulton R, Garcia ACL, Gardiner A, Garfield DA, Garvin BE, Gibson G, Gilbert D, Gnerre S, Godfrey J, Good R, Gotea V, Gravely B, Greenberg AJ, Griffiths-Jones S, Gross S, Guigo R, Gustafson EA, Haerty W, Hahn MW, Halligan DL, Halpern AL, Halter GM, Han MV, Heger A, Hillier L, Hinrichs AS, Holmes I, Hoskins RA, Hubisz MJ, Hultmark D, Huntley MA, Jagadeeshan S, Jeck WR, Johnson J, Jones CD, Jordan WC, Karpen GH, Kataoka E, Keightley PD, Kheradpour P, Kirkness EF, Koerich LB, Kristiansen K, Kudrna D, Kulathinal RJ, Kumar S, Kwok R, Lander E, Langley CH, Lapoint R, Lazzaro BP, Lee S-J, Levesque L, Li R, Lin C-F, Lin MF, Lindblad-Toh K, Llopart A, Long M, Low L, Lozovsky E, Lu J, Luo M, Machado CA, Makalowski W, Marzo M, Matsuda M, Matzkin L, McAllister B, McBride CS, McKernan B, McKernan K, Mendez-Lago M, Minx P, Mollenhauer MU, Montooth K, Mount SM, Mu X, Myers E, Negre B, Newfeld S, Nielsen R, Noor MAF, O'Grady P, Pachter L, Papaceit M, Parisi MJ, Parisi M, Parts L, Pedersen JS, Pesole G, Phillippy AM, Ponting CP, Pop M, Porcelli D, Powell JR, Prohaska S, Pruitt K, Puig M, Quesneville H, Ram KR, Rand D, Rasmussen MD, Reed LK, Reenan R, Reily A, Remington KA, Rieger TT, Ritchie MG, Robin C, Rogers Y-H, Rohde C, Rozas J, Rubenfield MJ, Ruiz A, Russo S, Salzberg SL, Sanchez-Gracia A, Saranga DJ, Sato H, Schaeffer SW, Schatz MC, Schlenke T, Schwartz R, Segarra C, Singh RS, Sirot L, Sirota M, Sisneros NB, Smith CD, Smith TF, Spieth J, Stage DE, Stark A, Stephan W, Strausberg RL, Strempel S, Sturgill D, Sutton G, Sutton GG, Tao W, Teichmann S, Tobari YN, Tomimura Y, Tsolas JM, Valente VLS, Venter E, Venter JC, Vicario S, Vieira FG, Vilella AJ, Villasante A, Walenz B, Wang J, Wasserman M, Watts T, Wilson D, Wilson RK, Wing RA, Wolfner MF, Wong A, Wong GK-S, Wu C-I, Wu G, Yamamoto D, Yang H-P, Yang S-P, Yorke JA, Yoshida K, Zdobnov E, Zhang P, Zhang Y, Zimin AV, Baldwin J, Abdouelleil A, Abdulkadir J, Abebe A, Abera B, Abreu J, Acer SC, Aftuck L, Alexander A, An P, Anderson E, Anderson S, Arachi H, Azer M, Bachantsang P, Barry A, Bayul T, Berlin A, Bessette D, Bloom T, Blye J, Boguslavskiy L, Bonnet C, Boukhgalter B, Bourzgui I, Brown A, Cahill P, Channer S, Cheshatsang Y, Chuda L, Citroen M, Collymore A, Cooke P, Costello M, D'Aco K, Daza R, De Haan G, DeGray S, DeMaso C, Dhargay N, Dooley K, Dooley E, Doricent M, Dorje P, Dorjee K, Dupes A, Elong R, Falk J, Farina A, Faro S, Ferguson D, Fisher S, Foley CD, Franke A, Friedrich D, Gadbois L, Gearin G, Gearin CR, Giannoukos G, Goode T, Graham J, Grandbois E, Grewal S, Gyaltsen K, Hafez N, Hagos B, Hall J, Henson C, Hollinger A, Honan T, Huard MD, Hughes L, Hurhula B, Husby ME, Kamat A, Kanga B, Kashin S, Khazanovich D, Kisner P, Lance K, Lara M, Lee W, Lennon N, Letendre F, LeVine R, Lipovsky A, Liu X, Liu J, Liu S, Lokyitsang T, Lokyitsang Y, Lubonja R, Lui A, MacDonald P, Magnisalis V, Maru K, Matthews C, McCusker W, McDonough S, Mehta T, Meldrim J, Meneus L, Mihai O, Mihalev A, Mihova T, Mittelman R, Mlenga V, Montmayeur A, Mulrain L, Navidi A, Naylor J, Negash T, Nguyen T, Nguyen N, Nicol R, Norbu C, Norbu N, Novod N, O'Neill B, Osman S, Markiewicz E, Oyono OL, Patti C, Phunkhang P, Pierre F, Priest M, Raghuraman S, Rege F, Reyes R, Rise C, Rogov P, Ross K, Ryan E, Settipalli S, Shea T, Sherpa N, Shi L, Shih D, Sparrow T, Spaulding J, Stalker J, Stange-Thomann N, Stavropoulos S, Stone C, Strader C, Tesfaye S, Thomson T, Thoulutsang Y, Thoulutsang D, Topham K, Topping I, Tsamla T, Vassiliev H, Vo A, Wangchuk T, Wangdi T, Weiand M, Wilkinson J, Wilson A, Yadav S, Young G, Yu Q, Zembek L, Zhong D, Zimmer A, Zwirko Z, Jaffe DB, Alvarez P, Brockman W, Butler J, Chin C, Grabherr M, Kleber M, Mauceli E, MacCallum I (2007) Evolution of genes and genomes on the *Drosophila* phylogeny. Nature 450(7167):203–218. doi:10.1038/nature06341

Counce SJ (1963) Developmental morphology of polar granules in *Drosophila* including observations on pole cell behavior and distribution during embryogenesis. J Morphol 112(2):129–145

Da Lage JL, Kergoat GJ, Maczkowiak F, Silvain FF, Cariou ML, Lachaise D (2006) A phylogeny of Drosophilidae using the *Amyrel* gene: questioning the *Drosophila melanogaster* species group boundaries. J Zool Syst Evol Res 45(1):47–63

Edgar RC (2004) MUSCLE: a multiple sequence alignment method with reduced time and space complexity. BMC Bioinforma 5:113. doi:10.1186/1471-2105-5-113

Ephrussi A, Lehmann R (1992) Induction of germ cell formation by *oskar*. Nature 358(6385):387–392

Ephrussi A, Dickinson LK, Lehmann R (1991) Oskar organizes the germ plasm and directs localization of the posterior determinant *nanos*. Cell 66(1):37–50

Ewen-Campen B, Schwager EE, Extavour CG (2010) The molecular machinery of germ line specification. Mol Reprod Dev 77(1):3–18

Ewen-Campen B, Srouji JR, Schwager EE, Extavour CG (2012) *oskar* predates the evolution of germ plasm in insects. Curr Biol 22(23):2278–2283

Extavour CG, Akam ME (2003) Mechanisms of germ cell specification across the metazoans: epigenesis and preformation. Development 130(24):5869–5884

Gaunt MW, Miles MA (2002) An insect molecular clock dates the origin of the insects and accords with palaeontological and biogeographic landmarks. Mol Biol Evol 19(5):748–761

Gharib WH, Robinson-Rechavi M (2013) The branch-site test of positive selection is surprisingly robust but lacks power under synonymous substitution saturation and variation in GC. Mol Biol Evol 30(7):1675–1686. doi:10.1093/molbev/mst062

Goltsev Y, Hsiong W, Lanzaro G, Levine M (2004) Different combinations of gap repressors for common stripes in *Anopheles* and *Drosophila* embryos. Dev Biol 275(2):435–446

Jones JR, Macdonald PM (2007) Oskar controls morphology of polar granules and nuclear bodies in *Drosophila*. Development 134(2):233–236

Juhn J, James AA (2006) oskar gene expression in the vector mosquitoes, *Anopheles gambiae* and *Aedes aegypti*. Insect Mol Biol 15(3):363–372

Juhn J, Marinotti O, Calvo E, James AA (2008) Gene structure and expression of *nanos* (*nos*) and *oskar* (*osk*) orthologues of the vector mosquito, *Culex quinquefasciatus*. Insect Mol Biol 17(5):545–552

Keller O, Kollmar M, Stanke M, Waack S (2011) A novel hybrid gene prediction method employing protein multiple sequence alignments. Bioinformatics 27(6):757–763. doi:10.1093/bioinformatics/btr010

Kopp A (2006) Basal relationships in the *Drosophila melanogaster* species group. Mol Phylogenet Evol 39(3):787–798. doi:10.1016/j.ympev.2006.01.029

Larracuente AM, Sackton TB, Greenberg AJ, Wong A, Singh ND, Sturgill D, Zhang Y, Oliver B, Clark AG (2008) Evolution of protein-coding genes in *Drosophila*. Trends Genet 24(3):114–123. doi:10.1016/j.tig.2007.12.001

Löytynoja A, Goldman N (2008) Phylogeny-aware gap placement prevents errors in sequence alignment and evolutionary analysis. Science (New York, NY) 320(5883):1632–1635. doi:10.1126/science.1158395

Lynch JA, Özüak O, Khila A, Abouheif E, Desplan C, Roth S (2011) The phylogenetic origin of *oskar* coincided with the origin of maternally provisioned germ plasm and pole cells at the base of the holometabola. PLoS Genet 7(4):e1002029. doi:10.1371/journal.pgen.1002029

Mahowald AP (1962) Fine structure of pole cells and polar granules in *Drosophila melanogaster*. J Exp Zool 151:201–215

Mahowald AP (1968) Polar granules of *Drosophila*. II. Ultrastructural changes during early embryogenesis. J Exp Zool 167(2):237–261. doi:10.1002/jez.1401670211

Markova-Raina P, Petrov D (2011) High sensitivity to aligner and high rate of false positives in the estimates of positive selection in the 12 *Drosophila* genomes. Genome Res 21(6):863–874. doi:10.1101/gr.115949.110

Markussen FH, Michon AM, Breitwieser W, Ephrussi A (1995) Translational control of *oskar* generates short OSK, the isoform that induces pole plasm assembly. Development 121(11):3723–3732

Michod RE (2005) On the transfer of fitness from the cell to the multicellular organism. Biol Philos 20(5):967–987

Obbard DJ, Maclennan J, Kim KW, Rambaut A, O'Grady PM, Jiggins FM (2012) Estimating divergence dates and substitution rates in the *Drosophila* phylogeny. Mol Biol Evol 29(11):3459–3473. doi:10.1093/molbev/mss150

Oliveira DCSG, Almeida FC, O'Grady PM, Armella MA, DeSalle R, Etges WJ (2012) Monophyly, divergence times, and evolution of host plant use inferred from a revised phylogeny of the *Drosophila repleta* species group. Mol Phylogenet Evol 64(3):533–544. doi:10.1016/j.ympev.2012.05.012

Privman E, Penn O, Pupko T (2012) Improving the performance of positive selection inference by filtering unreliable alignment regions. Mol Biol Evol 29(1):1–5. doi:10.1093/molbev/msr177

Remsen J, O'Grady P (2002) Phylogeny of Drosophilinae (Diptera: Drosophilidae), with comments on combined analysis and character support. Mol Phylogenet Evol 24(2):249–264

Robe LJ, Valente VLS, Budnik M, Loreto ELS (2005) Molecular phylogeny of the subgenus *Drosophila* (Diptera, Drosophilidae) with an emphasis on Neotropical species and groups: a nuclear versus mitochondrial gene approach. Mol Phylogenet Evol 36(3):623–640. doi:10.1016/j.ympev.2005.05.005

Rongo C, Gavis ER, Lehmann R (1995) Localization of *oskar* RNA regulates *oskar* translation and requires Oskar protein. Development 121(9):2737–2746

Sayle RA, Milner-White EJ (1995) RASMOL: biomolecular graphics for all. Trends Biochem Sci 20(9):374

Studer RA, Penel S, Duret L, Robinson-Rechavi M (2008) Pervasive positive selection on duplicated and nonduplicated vertebrate protein coding genes. Genome Res 18(9):1393–1402. doi:10.1101/gr.076992.108

Suyama R, Jenny A, Curado S, Pellis-van Berkel W, Ephrussi A (2009) The actin-binding protein Lasp promotes Oskar accumulation at the posterior pole of the *Drosophila* embryo. Development 136(1):95–105. doi:10.1242/dev.027698

Tamura K, Subramanian S, Kumar S (2004) Temporal patterns of fruit fly (*Drosophila*) evolution revealed by mutation clocks. Mol Biol Evol 21(1):36–44. doi:10.1093/molbev/msg236

van der Linde K, Houle D, Spicer GS, Steppan SJ (2010) A supermatrix-based molecular phylogeny of the family Drosophilidae. Genet Res 92(1):25–38

Vanzo NF, Ephrussi A (2002) Oskar anchoring restricts pole plasm formation to the posterior of the *Drosophila* oocyte. Development 129(15):3705–3714

Vanzo N, Oprins A, Xanthakis D, Ephrussi A, Rabouille C (2007) Stimulation of endocytosis and actin dynamics by Oskar polarizes the *Drosophila* oocyte. Dev Cell 12(4):543–555

Webster PJ, Suen J, Macdonald PM (1994) *Drosophila virilis oskar* transgenes direct body patterning but not pole cell formation or maintenance of mRNA localization in *D. melanogaster*. Development 120(7):2027–2037

Yang Z (2007) PAML 4: phylogenetic analysis by maximum likelihood. Mol Biol Evol 24(8):1586–1591. doi:10.1093/molbev/msm088

Yang Z, Swanson WJ (2002) Codon-substitution models to detect adaptive evolution that account for heterogeneous selective pressures among site classes. Mol Biol Evol 19(1):49–57

Yang Z, Nielsen R, Goldman N, Pedersen AM (2000a) Codon-substitution models for heterogeneous selection pressure at amino acid sites. Genetics 155(1):431–449

Yang Z, Swanson WJ, Vacquier VD (2000b) Maximum-likelihood analysis of molecular adaptation in abalone sperm lysin reveals variable selective pressures among lineages and sites. Mol Biol Evol 17(10):1446–1455

Yang Z, Wong WS, Nielsen R (2005) Bayes empirical Bayes inference of amino acid sites under positive selection. Mol Biol Evol 22(4):1107–1118. doi:10.1093/molbev/msi097

Yang Y, Hou Z-C, Y-h Q, Kang H, Zeng Q-t (2012) Increasing the data size to accurately reconstruct the phylogenetic relationships between nine subgroups of the *Drosophila melanogaster* species group (*Drosophilidae, Diptera*). Mol Phylogenet Evol 62(1):214–223. doi:10.1016/j.ympev.2011.09.018

Zhang J, Nielsen R, Yang Z (2005) Evaluation of an improved branch-site likelihood method for detecting positive selection at the molecular level. Mol Biol Evol 22(12):2472–2479. doi:10.1093/molbev/msi237